

Photoelectroenzymatic Oxyfunctionalization on Flavin-Hybridized Carbon Nanotube Electrode Platform

Choi, Da Som; Ni, Yan; Fernández-Fueyo, Elena; Lee, Minah; Hollmann, Frank; Park, Chan Beum

DOI

[10.1021/acscatal.6b03453](https://doi.org/10.1021/acscatal.6b03453)

Publication date

2017

Document Version

Accepted author manuscript

Published in

ACS Catalysis

Citation (APA)

Choi, D. S., Ni, Y., Fernández-Fueyo, E., Lee, M., Hollmann, F., & Park, C. B. (2017). Photoelectroenzymatic Oxyfunctionalization on Flavin-Hybridized Carbon Nanotube Electrode Platform. *ACS Catalysis*, 7(3), 1563-1567. <https://doi.org/10.1021/acscatal.6b03453>

Important note

To cite this publication, please use the final published version (if applicable). Please check the document version above.

Copyright

Other than for strictly personal use, it is not permitted to download, forward or distribute the text or part of it, without the consent of the author(s) and/or copyright holder(s), unless the work is under an open content license such as Creative Commons.

Takedown policy

Please contact us and provide details if you believe this document breaches copyrights. We will remove access to the work immediately and investigate your claim.

Photoelectroenzymatic oxyfunctionalization on flavin-hybridized carbon nanotube electrode platform

Da Som Choi,[†] Yan Ni,[‡] Elena Fernández-Fueyo,[‡] Minah Lee,[†] Frank Hollmann,^{*,‡} and Chan Beum Park^{*,†}

[†] Department of Materials Science and Engineering, Korea Advanced Institute of Science and Technology, Daejeon 305–701, Republic of Korea.

[‡] Department of Biotechnology, Delft University of Technology, Van der Maasweg 9, 2629HZ Delft, The Netherlands.

ABSTRACT: Peroxygenases are very promising catalysts for oxyfunctionalization reactions. Their practical applicability, however, is hampered by their sensitivity against the oxidant (H₂O₂), therefore necessitating *in situ* generation of H₂O₂. Here, we report a photoelectrochemical approach to provide peroxygenases with suitable amounts of H₂O₂ while reducing the electrochemical overpotential needed for the reduction of molecular oxygen to H₂O₂. When tethered on single-walled carbon nanotubes (SWNT) under illumination, flavins allowed for a marked anodic shift of the oxygen reduction potential in comparison to pristine-SWNT and/or non-illuminated electrodes. This flavin-SWNT-based photoelectrochemical platform enabled peroxygenases-catalyzed, selective hydroxylation reactions.

KEYWORDS: heme proteins, oxyfunctionalization, photoelectrochemistry, flavins, peroxygenases

Peroxygenases are versatile catalysts for specific oxyfunctionalization reactions even on non-activated C-H bonds.^{1,2} Unlike cytochrome P450 monooxygenases that depend on complicated and vulnerable electron-transport chains for reductive activation of molecular oxygen, peroxygenases utilize H₂O₂ directly to form the catalytically active oxyferryl-heme species. This inherent advantage results in significantly simplified reaction schemes, making peroxygenases promising catalysts for organic oxyfunctionalization chemistry on a preparative scale. Despite the high potential of peroxygenases, however, their practical application is hampered by their poor operational stability towards H₂O₂, which causes oxidative degradation of catalytic heme moiety. Typically, this challenge has been met by *in situ* provision of peroxygenases with suitable amounts of H₂O₂ by catalytic reduction of molecular oxygen using chemical,^{3,4} electrochemical,^{5–8} photochemical,^{9–11} or enzymatic methods.^{12–16} Electrochemical H₂O₂ supply is an attractive approach with no need of additional catalyst for H₂O₂ generation, avoiding the accumulation of byproducts in the reaction mixture. A few studies have been reported for electrochemical reduction of O₂ using gas diffusion electrode (GDE) or carbon-based electrodes.^{5–8} Due to kinetic limitations, however, simple, non-modified carbon electrodes require significant overpotentials to attain efficient O₂-reduction rates, resulting in additional energy expenditures.

Here, we report flavin-hybridized, single-walled carbon nanotube (SWNT) photoelectrodes for *in situ* generation of H₂O₂ to promote peroxygenase-catalysis at low applied potential, as depicted in **Figure 1**. Flavins are made of a heterocyclic conjugated ring structure (i.e., isoalloxazine ring) (**Figure S1a**), which are vital compounds for diverse redox reactions in living organisms. Flavins undergo reversible redox conversion,

involving N(1) and N(5) of the isoalloxazine ring (**Figure S1b**). Reduced flavins are well-known to react swiftly with molecular oxygen in a diffusion-controlled manner, yielding oxidized flavins and hydrogen peroxide.¹⁷ Furthermore, flavins are excellent photosensitizers that absorb visible light at around 450 nm. Upon illumination, photoexcited flavins exhibit a

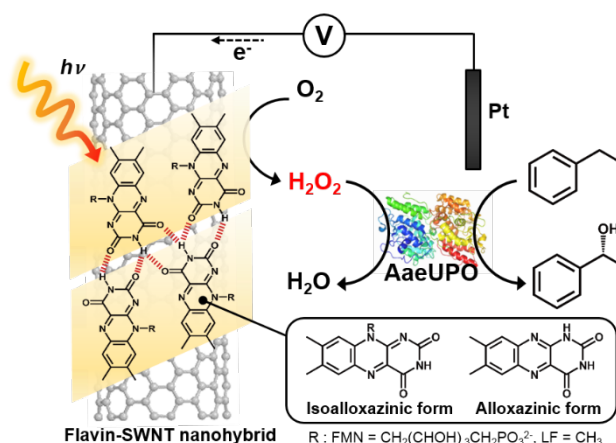


Figure 1. Schematic illustration of photoelectrochemical generation of H₂O₂ for peroxygenase catalysis. AaeUPO catalyzes the chemo- and stereospecific conversion of ethylbenzene to (R)-1-phenylethanol. In situ provision of H₂O₂ is achieved via reduction of oxygen by using flavin-SWNT electrodes under illumination.

more positive redox potential (E⁰, ³Fl[•]/Fl, +1.85 V) than the ground state flavins (E⁰, Fl/Fl⁻, -0.22 V) and their electron affinity is significantly enhanced;¹⁸ hence, photoexcited flavins appear to be interesting co-catalysts to facilitate charge

transfer to molecular oxygen from the cathode by reducing the overpotential of O₂ reduction (**Figure S2**).

To utilize flavins for photoelectrocatalytic H₂O₂ generation, SWNTs were chosen as a scaffold to anchor flavin molecules because of their good chemical stability, high surface area, and superb electrical and mechanical properties.¹⁹ Flavins can be easily immobilized on the surface of SWNT electrodes via a simple hybridization process while maintaining their redox-active properties.^{20,21} The hybridization of flavins with SWNTs occurs through π - π interactions between aromatic isoalloxazine moieties and graphitic carbons in addition to hydrogen bonds between adjacent flavin molecules.

We investigated three different types of flavin molecules—flavin mononucleotide (FMN), lumiflavin (LF), and lumichrome (LC)—for their abilities to anchor on the surface of SWNTs and photoelectrocatalytic activity for O₂ reduction. We have chosen these flavin derivatives because of their high photostability compared to other flavin molecules.²² A highly conductive flavin-SWNT film electrode was synthesized by sonicating a suspension of flavin powder (1 mg) and SWNTs (5 mg) in a suitable organic solvent (acetone for LF and LC,

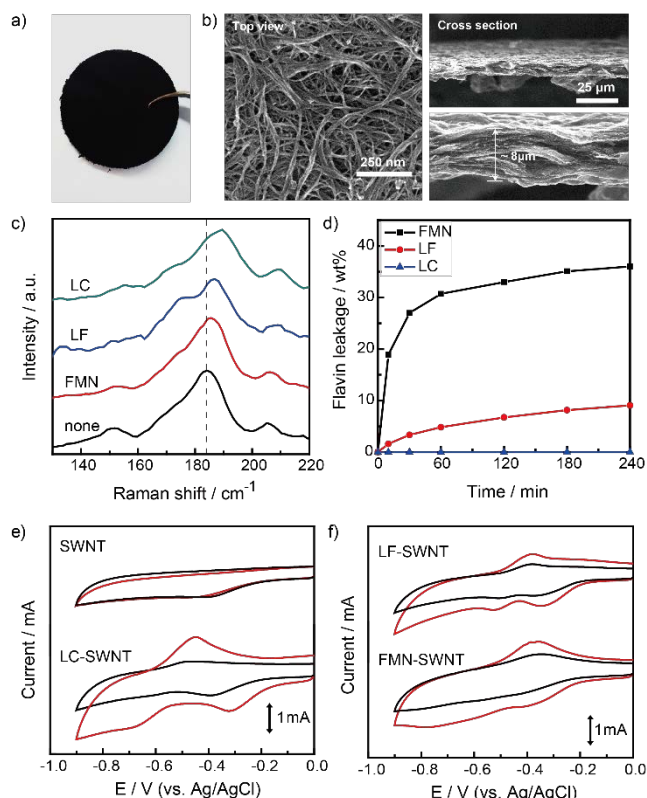


Figure 2. (a) Pictures and (b) SEM images of LC-SWNT nanohybrid. (c) The Radial Breathing Modes (RBMs) of pristine SWNT and flavin-SWNT electrodes at laser excitation of 514.5 nm. Red shifting of RBMs for flavin-SWNT indicates the π - π interaction between SWNTs and flavin molecules. (d) Time profiles of the weight percentage of flavin (FMN, LF and LC) leaked out of the electrode. Each electrode was immersed in 3ml of DI water. (e), (f) CVs for oxygen reduction at the pristine SWNT and flavin-SWNT electrodes in the O₂-saturated phosphate buffer (100 mM, pH 7.0) at 25°C in the dark (black curves) and under visible-light illumination (red curves). Scan rate 25mVs⁻¹. All electrodes had geometrical surface area of 1 cm².

ethanol for FMN) for 7 h, followed by vacuum filtration (**Figure 2a**). As a result of the hybridization, flavin molecules were reconstructed from crystalline particles to a nanoscale ad-layer on the surface of SWNT scaffold that formed an

intertwined network structure (**Figure 2b**). According to our analysis of flavin contents by N concentrations in the nanocomposite using an organic elemental analyzer, 11.5 wt% (FMN), 13.8 wt% (LF), and 12.3 wt% (LC) were loaded to each hybrid electrode. We observed the interaction between the surface of SWNTs and flavin molecules using Raman spectroscopy (**Figure 2c**). A higher frequency shift (\sim 5 cm⁻¹) of the radial breathing mode peak at 184 cm⁻¹ was observed in all samples, which is contributed to the π - π interactions between SWNTs and flavin molecules. We examined possible leaching of the flavin molecules from the SWNT surface by immersing them in deionized water (**Figure 2d**). After 4 h of incubation, approximately 36% of FMN and 9% of LF molecules diffused into the aqueous solution, while LC remained intact on the SWNTs due to its hydrophobicity. We attribute the significant leaching of FMN to its hydrophilic ribityl phosphate residue that interacts with water molecules.

We evaluated O₂-reduction activities of the flavin-SWNT electrodes in a O₂-saturated solution under light-on and -off conditions by cyclic voltammetric analysis. As shown in **Figures 2e** and **2f**, the currents for O₂ reduction were enhanced by the presence of flavin redox catalysts upon light irradiation. The current increase should be caused by photoexcited flavins that convert to their reduced form by accepting electrons from the cathode and consequently transfer the electrons to dissolved oxygen during their aerobic reoxidation pathways.¹⁷ Such cathodic waves did not form under anaerobic conditions (**Figure S3**), which confirms that the peaks stemmed from O₂ reduction. Under light illumination, the value of O₂ reduction peak potential for LC-SWNT electrodes was -0.32 V (vs Ag/AgCl), which was more anodic than that observed in the same experiment conducted under dark condition (-0.4 V vs Ag/AgCl). Also, the current density markedly increased from -0.84 mA cm⁻² to -1.42 mA cm⁻² with light illumination. We also characterized the photoresponsive behavior of LC-SWNT by measuring photocurrent changes at a potential of -0.3 V (vs. Ag/AgCl) with chopped illumination (**Figure S4**). We found that the maximum values of cathodic current at LF-SWNT and FMN-SWNT electrodes under light conditions were approximately -1.04 mA cm⁻² (at -0.35 V) and -1.23 mA cm⁻² (at -0.43 V), respectively. They exhibited pronounced performances for O₂ reduction compared to pristine SWNT (-0.49 V vs Ag/AgCl, -0.87 mA cm⁻²), but their O₂ reduction overpotentials were still higher than that of LC-SWNT, which is attributed to their unstable binding to the surface of SWNTs; thus, we selected LC as a model flavin in this work because it was most active toward O₂ reduction and firmly bound to the surface of SWNTs without leaching to aqueous solution. LC has an alloxazinic structure, different from common flavins. Previous studies on LC observed the tautomerization from the alloxazinic type to an isoalloxazinic one during electrochemical reduction process (**Figure S1c**).²³ In the current system, likewise, LC should readily tautomerize to more stable form during redox reactions.

Figure 3 shows such beneficial characteristics of LC-SWNT in potentiostatic electrolysis. Under a cell voltage of -0.3 V (vs Ag/AgCl) with light illumination, H₂O₂ was produced with a rate of 0.15 mM h⁻¹, which is 2.28- and 2.48-fold higher than control experiments without light or using a pristine SWNT cathode under light, respectively. The individual time courses are shown in **Figure S5**. The highest current efficiency of 58 % was detected at LC-SWNT electrode under illumination. The results indicate that an efficient production of H₂O₂ at LC-SWNT photoelectrode was achieved while minimizing undesirable side reactions^{24,25} such as chemical

decomposition of H_2O_2 to O_2 and further reduction of H_2O_2 to H_2O . Possibly, in these experiments oxygen availability became overall rate-limiting due to the poor solubility of molecular O_2 in aqueous media (ca. 0.25 mM at 20°C) and its rapid depletion at the cathode surface. Therefore, we bubbled O_2 gas into electrolyte solution through a Teflon tube (2 mm diameter) and found that H_2O_2 formation rate increased remarkably to 0.37 mM h^{-1} . In all further experiments, O_2 feed was applied because of the reason.

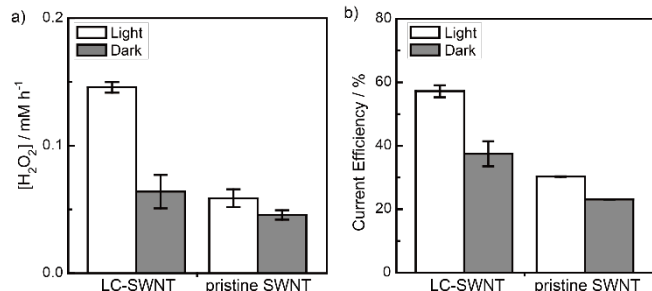


Figure 3. (a) H_2O_2 formation rate and (b) current efficiency with LC-SWNT and pristine SWNT electrode in phosphate buffer (100 mM, pH 7.0) at -0.3 V (vs. Ag/AgCl) under illumination and in the dark. T = 25°C. All electrodes had geometrical surface area of 1 cm^2 .

Next, we coupled the photoelectrochemical *in situ* H_2O_2 generation platform with peroxygenase-driven catalysis to perform oxyfunctionalization reactions. We chose heme-thiolate peroxygenase from *Agrocybe aegerita* (*AaeUPO*, E.C.1.11.2.1)²⁶⁻²⁸ as a model enzyme to catalyze the enantioselective hydroxylation of ethylbenzene to (*R*)-1-phenylethanol. *AaeUPO* is a promising biocatalyst to replace P450 monooxygenases because of its high towards (non-)activated $\text{C}(\text{sp}^3)\text{-H}$ bonds.¹ To characterize the production of (*R*)-1-phenylethanol, we investigated the effects of key reaction parameters such as applied voltage and flavin concentration in hybridization media. The reaction was carried out in one pot reactor, consisting of a LC-SWNT cathode (with the geometric surface area of 1 cm^2) and a platinum anode, with the reaction volume of 2 mL while bubbling O_2 into the reaction medium. **Figure 4a** displays the product formation rate during 4 h as a function of the applied potential ranging from -0.2 to -0.5 V (vs. Ag/AgCl). Note that, in all cases, enantiopure products (ee > 99%) were obtained while no product was detected at below -0.1 V potential or in the absence of *AaeUPO* or with denatured *AaeUPO* under light conditions (data not shown). The product formation rate achieved a maximum value of 0.72 mM h^{-1} at an applied potential of -0.4 V and decreased at -0.5 V. This decrease may be caused by the loss of enzyme activity. The accumulation of reactive oxygen species (ROS) such as superoxide radical anion and hydroxyl radical may occur at higher voltage applied, leading to oxidative degradation of the heme and/or amino acid residues. Note that the product formation rates under illumination are higher than that in the dark except at -0.2 V. These results prove that light has a beneficial effect on *AaeUPO*-catalyzed hydroxylation in this system. We found that the flavin amount loaded to the electrode was another factor affecting the photoelectroenzymatic process. According to our observation (**Figure 4b**), 13 wt% LC-containing electrode showed the highest rate of *AaeUPO* catalyzed reaction (0.72 mM h^{-1}), which was two-fold higher that of bare SWNT electrode. At above 13 wt% of LC content, product formation rates decreased. We attribute the result to the precipitation of excess LC molecules as disordered particles on the hybrids

that impede electrical flow between SWNT and LC molecules and thus lead to low productivity (**Figure S6**). We further tested the stability of the flavin-SWNT electrode-based reaction system. **Figure 4c, 4d** shows the time-dependent profile of *AaeUPO*-catalyzed hydrogenation of ethylbenzene using the same LC-SWNT electrode. The linearly increasing product formation demonstrates that stable operational activity of *AaeUPO* sustained by exploiting low H_2O_2 level in the system. Overall, ethylbenzene was converted into (*R*)-1-phenylethanol of 17 mM and acetophenone (originating from *AaeUPO*-catalyzed oxidation of the primary product) of 3 mM as the sole side product. Optical purities of the final products were approximately 95% ee. We confirmed that the electrode could be reused (more than thrice) without any appreciable activity reduction. Also, the current density of the working electrode remained stable at $\sim 100 \mu\text{A cm}^{-2}$ for electrolysis over 40 h (**Figure S7**). This exceptional durability shows a promise for practical applications of the LC-SWNT hybrid electrode.

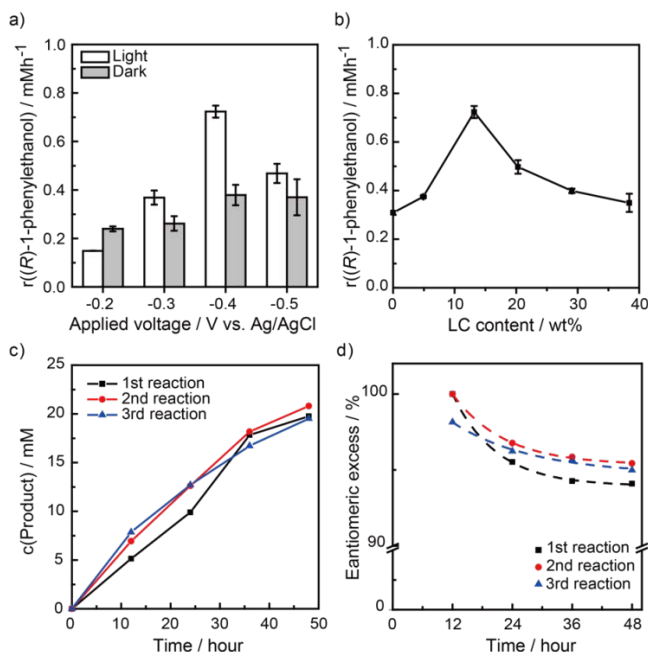
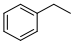
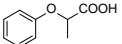
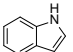


Figure 4. The effect of (a) applied voltage and (b) LC content (wt%) on the photoelectroenzymatic formation rate of (*R*)-1-phenylethanol. Time courses of hydroxylation of ethylbenzene with respect to (c) yield and (d) optical purity of the product during repetitive experiments. After use the electrode was washed, dried at room temperature and used for reaction. 100 mM substrate was added after each sampling because of the technical issue of substrate evaporation. Reaction conditions: 100 mM phosphate buffer (pH 7.0, 2 mL) containing 200 nM *AaeUPO* and 100 mM ethylbenzene; -0.4 V (vs Ag/AgCl); 25°C.

To investigate general applicability of the LC-SWNT photoelectrocatalytic system, we tested other peroxygenase-catalyzed reactions: (1) *AaeUPO* for hydroxylation of 2-phenoxypropanoic acid and (2) chloroperoxidases from *Caldariomyces fumago* (CPO)²⁹ for indole oxidation, which also exhibits poor operational stability towards H_2O_2 . **Table 1** summarizes the turnover number (TON) and space-time-yield (STY) of the different reactions. The TON and STY values were calculated at the end of each process, where no further conversion of substrate was observed. The conversion of ethylbenzene showed the highest TON of over 123,000, while TONs for *AaeUPO*-catalyzed 2-phenoxypropanoic acid hydroxylation and CPO-catalyzed indole oxidation were 5,900 and 4,900, respectively. In the case of CPO, the TON and STY

could be improved by further optimization of reaction conditions to stabilize enzyme, e.g. using a cosolvent act as a radical scavenger such as *tert*-butanol.^{6,30} The successful application of LC-SWNT photoelectrocatalytic system to other peroxygenase-catalyzed reactions signify that the reaction setup is not limited to the stereospecific hydroxylation of ethylbenzene but also could be extended to a representative range of peroxygenase-catalyzed reactions.

Table 1. Peroxygenase-catalyzed reactions driven by the proposed photoelectrochemical in situ H₂O₂ generation approach^a

Enzyme	Substrate	TON (mol product mol enzyme ⁻¹)	STY (g L ⁻¹ d ⁻¹)
AaeUPO ^b		123,900 ± 7,290	1.00 ± 0.06
AaeUPO ^c		5,900 ± 210	0.13 ± 0.01
CPO ^d		4,900 ± 340	0.88 ± 0.06

^aAll the values are an average of at least three independent reactions with standard deviation. ^b[AaeUPO]=100 nM, [ethylbenzene]=100 mM in a phosphate buffer (100 mM, pH 7.0), 25°C. During the reaction ethylbenzene was added to prevent substrate limitations. ^c[AaeUPO]=200 nM, [2-phenoxypropionic acid]=10 mM in a phosphate buffer (100 mM, pH 7.0), 25°C. ^d[CPO]=1 μM, [indole]=10 mM in a phosphate buffer (50 mM, pH 5.1), 30°C.

In summary, we have demonstrated the first photoelectrochemical approach for *in situ* H₂O₂ generation using flavin-SWNT electrode to promote peroxygenase-catalyzed reactions. Oxygen reduction activity greatly enhanced by the flavin photosensitizers such as LC incorporated into the SWNT network. Under visible light illumination, LC reduced the overpotential for oxygen reduction by 170 mV when compared to the pristine SWNT electrode. This overpotential reduction is attributed to the facilitated electron transfer to oxygen by photoexcited LC. We optimized the reaction parameters (e.g., applied potential, LC concentration) were optimized to observe an efficient photoelectroenzymatic hydroxylation of ethylbenzene with the TON of 123,900. Compared to established methods, our approach do not require sacrificial electron donors, avoiding the accumulation of by-products and, takes advantage of applying low potential to realize energy-efficient synthesis of H₂O₂. The flavin-SWNT system serves as a suitable platform technology for the application of a wide range of peroxygenases for fine and specialty chemical production.

ASSOCIATED CONTENT

Supporting Information: Experimental details, proposed mechanism for photoelectrochemical H₂O₂ generation, cyclic voltammograms in the N₂-saturated buffer, additional SEM images, and time course of current density during ethylbenzene hydroxylation (PDF)

AUTHOR INFORMATION

Corresponding Authors

*E-mail for C.B.P.: parkcb@kaist.ac.kr.

*E-mail for F.H.: f.hollmann@tudelft.nl.

Notes

The authors declare no competing financial interest.

ACKNOWLEDGMENT

This work was supported by the National Research Foundation (NRF) via the Creative Research Initiative Center (Grant number: NRF-2015 R1A3A2066191), Republic of Korea, for CBP and the Netherlands Organisation for Scientific Research by a VICI grant (Grant number: 724.014.003) for FH.

REFERENCES

- (1) Bormann, S.; Gomez Baraibar, A.; Ni, Y.; Holtmann, D.; Hollmann, F. *Catal. Sci. Technol.* **2015**, *5*, 2038-2052.
- (2) Hofrichter, M.; Ullrich, R. *Curr. Opin. Chem. Biol.* **2014**, *19*, 116-125.
- (3) Karmee, S. K.; Roosen, C.; Kohlmann, C.; Lutz, S.; Greiner, L.; Leitner, W. *Green Chem.* **2009**, *11*, 1052-1055.
- (4) Paul, C. E.; Churakova, E.; Maurits, E.; Girhard, M.; Urlacher, V. B.; Hollmann, F. *Bioorgan. Med. Chem.* **2014**, *22*, 5692-5696.
- (5) Lütz, S.; Steckhan, E.; Liese, A. *Electrochem. Commun.* **2004**, *6*, 583-587.
- (6) Lütz, S.; Vuorilehto, K.; Liese, A. *Biotechnol. Bioeng.* **2007**, *98*, 525-534.
- (7) Krieg, T.; Hüttmann, S.; Mangold, K.-M.; Schrader, J.; Holtmann, D. *Green Chem.* **2011**, *13*, 2686-2689.
- (8) Getrey, L.; Krieg, T.; Hollmann, F.; Schrader, J.; Holtmann, D. *Green Chem.* **2014**, *16*, 1104-1108.
- (9) Perez, D. I.; Grau, M. M.; Arends, I. W. C. E.; Hollmann, F. *Chem. Commun.* **2009**, 6848-6850.
- (10) Churakova, E.; Kluge, M.; Ullrich, R.; Arends, I.; Hofrichter, M.; Hollmann, F. *Angew. Chem. Int. Ed.* **2011**, *50*, 10716-10719.
- (11) Churakova, E.; Arends, I. W. C. E.; Hollmann, F. *Chem-CatChem* **2013**, *5*, 565-568.
- (12) Ni, Y.; Fernandez-Fueyo, E.; Baraibar, A. G.; Ullrich, R.; Hofrichter, M.; Yanase, H.; Alcalde, M.; van Berkel, W. J. H.; Hollmann, F. *Angew. Chem. Int. Ed.* **2016**, *55*, 798-801.
- (13) van de Velde, F.; Lourenco, N. D.; Bakker, M.; van Rantwijk, F.; Sheldon, R. A. *Biotechnol. Bioeng.* **2000**, *69*, 286-291.
- (14) Pricelius, S.; Ludwig, R.; Lant, N. J.; Haltrich, D.; Guebitz, G. M. *Biotechnol. J.* **2011**, *6*, 224-230.
- (15) Okrasa, K.; Falcimaigne, A.; Guibé-Jampel, E.; Therisod, M. *Tetrahedron: Asymmetry* **2002**, *13*, 519-522.
- (16) Pezzotti, F.; Therisod, M. *Tetrahedron: Asymmetry* **2007**, *18*, 701-704.
- (17) Massey, V. *J. Biol. Chem.* **1994**, *269*, 22459-22462.
- (18) De La Rosa, M. A.; Navarro, J. A.; Roncel, M. *Appl. Biochem. Biotech.* **1991**, *30*, 61-81.
- (19) Popov, V. *Mater. Sci. Eng. R* **2004**, *43*, 61-102.
- (20) Ju, S. Y.; Doll, J.; Sharma, I.; Papadimitrakopoulos, F. *Nat. Nanotechnol.* **2008**, *3*, 356-362.
- (21) Lee, M.; Hong, J.; Kim, H.; Lim, H. D.; Cho, S. B.; Kang, K.; Park, C. B. *Adv. Mater.* **2014**, *26*, 2558-2565.
- (22) Song, S. H.; Dick, B.; Penzkofer, A. *Chem. Phys.* **2007**, *332*, 55-65.
- (23) Hong, J.; Lee, M.; Lee, B.; Seo, D. H.; Park, C. B.; Kang, K. *Nat. Commun.* **2014**, *5*, 5335.
- (24) Panizza, M.; Cerisola, G. *Electrochim. Acta* **2008**, *54*, 876-878.
- (25) Khataee, A. R.; Safarpour, M.; Zarei, M.; Aber, S. *J. Electroanal. Chem.* **2011**, *659*, 63-68.
- (26) Ullrich, R.; Nuske, J.; Scheibner, K.; Spantzel, J.; Hofrichter, M. *Appl. Environ. Microbiol.* **2004**, *70*, 4575-4581.
- (27) Molina-Espeja, P.; Garcia-Ruiz, E.; Gonzalez-Perez, D.; Ullrich, R.; Hofrichter, M.; Alcalde, M. *Appl. Environ. Microbiol.* **2014**, *80*, 3496-3507.
- (28) Molina-Espeja, P.; Ma, S.; Mate, D. M.; Ludwig, R.; Alcalde, M. *Enzyme Microb. Technol.* **2015**, *73-74*, 29-33.
- (29) Morris, D.R.; Hager, L.P. *J. Biol. Chem.* **1966**, *241*, 1763-1768.
- (30) Seelbach, K.; van Deurzen, M. P. J.; van Rantwijk, F.; Sheldon, R. A. *Biotechnol. Bioeng.* **1997**, *55*, 283-288.

Table of Contents (TOC)

